Behavior of Human Cytochromes P450 on Lipid Membranes

ARTICLE *in* THE JOURNAL OF PHYSICAL CHEMISTRY B · AUGUST 2013

Impact Factor: 3.3 · DOI: 10.1021/jp4059559 · Source: PubMed

4 AUTHORS, INCLUDING:

Karel Berka
Palacký University of Olomouc
49 PUBLICATIONS **666** CITATIONS
SEE PROFILE

Michal Otyepka
Palacký University of Olomouc
180 PUBLICATIONS **4,542** CITATIONS
SEE PROFILE

THE JOURNAL OF PHYSICAL CHEMISTRY B

Article

pubs.acs.org/JPCB

Behavior of Human Cytochromes P450 on Lipid Membranes

Karel Berka,[†] Markéta Paloncýová,[†] Pavel Anzenbacher,[‡] and Michal Otyepka*[,†]

[†]Department of Physical Chemistry, Regional Centre of Advanced Technologies and Materials, Faculty of Science, Palacký University Olomouc, tř. 17. listopadu 12, 771 46, Olomouc, Czech Republic

[‡]Department of Pharmacology, Faculty of Medicine and Dentistry, Palacký University Olomouc, Hněvotínská 3, 775 15 Olomouc, Czech Republic

Supporting Information

ABSTRACT: Human cytochromes P450 (CYPs) are membrane-anchored enzymes involved in biotransformation of many marketed drugs. We constructed atomic models of six human CYPs (CYP1A2, 2A6, 2C9, 2D6, 2E1, and 3A4) anchored to a lipid bilayer to investigate the positions and orientations of CYPs on a membrane. We equilibrated the models by molecular dynamics simulations on a 100+ ns time scale. Catalytic domains of all studied CYPs were found to be partially immersed in the lipid bilayer, whereas the N-terminal part and F′/G′ loop are deeply immersed. The proximal side of the enzyme faces the cytosol, whereas the distal side, where openings of substrate access and product release channels to the active site are primarily located, points toward the lipid bilayer. Access channels with openings in the vicinity of the B/C and F/G loops are typically positioned below the lipid head groups, whereas the solvent channel points toward the membrane–water interface. We found that the access channel opening positions match the preferred substrate positions, whereas the product release channel exit positions correspond closely with the positions of the products. This may indicate that membrane-anchored CYPs have evolutionarily adapted to facilitate uptake of nonpolar substrates from the membrane and uptake/release of polar substrates or products from/to the membrane–water interface.

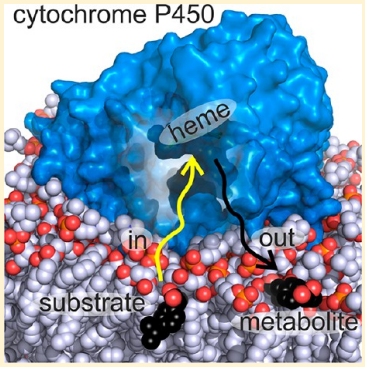

INTRODUCTION

Mammalian cytochromes P450 (CYPs) are involved in the metabolism of many endogenous compounds as well as xenobiotics. CYPs are attached to the endoplasmic reticulum or inner mitochondrial membranes via their N-terminal anchors.[1] The N-terminal anchor usually adopts an α-helical structure and is connected to the CYP catalytic domain via a loop. The fold of the catalytic domain is known from numerous X-ray experiments,[2−5] and its shape has been shown to be conserved over the mammalian CYPs.[6] It is expected that the majority of the catalytic domain is exposed to cytosol. However, the exact immersion (penetration depth) and orientation of CYPs on membranes remains uncertain. The orientations of some CYPs have been deduced from experimental data, e.g., epitope screening,[1,7,8] tryptophan fluorescence,[9,10] AFM experiments,[11,12] protein rotation,[13] linear dichroism,[14] etc. However, despite providing some basic information about the behavior of CYPs on a membrane, these experiments did not allow construction of an atomic model to predict the CYP orientation on the membrane. Recently, several groups have published atomic models of CYP2C9,[15,16] CYP3A4,[14,17] and human aromatase CYP19[18,19] positioned on a phosphatidylcholine lipid bilayer based on molecular dynamics simulations. All models have indicated that the CYP catalytic domain is partially immersed in the lipid bilayer, but the majority of the catalytic domain remains exposed to the cytosol. In addition, it has been predicted that the N-terminal anchor is immersed in the lipid bilayer and lies almost perpendicular to the bilayer surface, with the N-terminal apex almost reaching the polar headgroup region of the opposite membrane leaflet (Figure 1).

In our previous work,[15] we showed that the orientation of the CYP2C9 catalytic domain on the dioleoylphosphatidylcholine (DOPC) lipid bilayer was tilted and its proximal side faced the cytosol, whereas the distal side was partially immersed in the membrane. Consequently, the entrances of the active site access channels were located in the vicinity of the F′/G′ loop (channels 2a, 2ac, 2f, and 4 according to Wade et al.'s nomenclature[21]) below the polar headgroup region of the lipid bilayer (i.e., below the polar membrane surface). On the other hand, the opening of the solvent channel lies above the membrane surface. The position of the F′/G′-loop channel (2ac, 2f) opening agreed with the preferred (energetically most favorable) position of ibuprofen (typical CYP2C9 substrate) in a DOPC membrane. Similarly, the opening of the solvent channel agreed with the preferred position of 3′-hydroxyibuprofen (product of CYP2C9 oxidation of ibuprofen). These findings may indicate that some channels are involved in the uptake of low polar substrates from the lipid bilayer, whereas others are involved in the release of the respective products to the cytosol.[15,22]

Recently, we have shown that selected prototypical CYP substrates (caffeine, chlorzoxazone, coumarin, ibuprofen, and

Received: June 17, 2013
Revised: August 29, 2013
Published: August 29, 2013

   dx.doi.org/10.1021/jp4059559 | J. Phys. Chem. B 2013, 117, 11556−11564

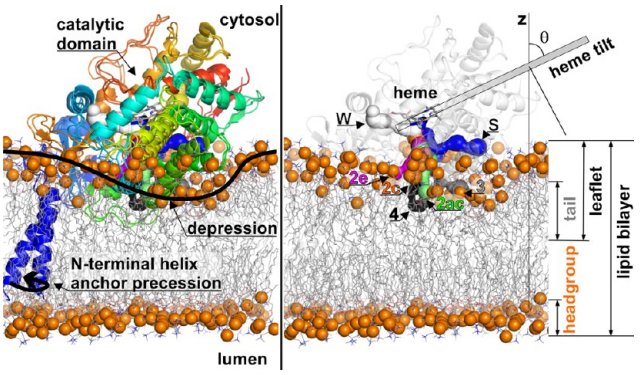

Figure 1. Immersion of CYP2C9 in a dioleoylphosphatidylcholine (DOPC) lipid bilayer. (Left) Overlaid snapshots of CYP2C9 taken at 0.1 and 1 μs molecular dynamics (MD) simulation, showing that the catalytic domain is immersed in a membrane depression framed by lipid phosphate groups (shown as orange spheres). Water molecules are not shown for clarity. N-terminal helix shows precessional movement about the bilayer normal. Fold of the catalytic domain is conserved and agrees with that observed in X-ray crystallography experiments. (Right) Snapshot taken at 1 μs of MD simulation showing positions of active site access and egress channels computed from the heme moiety using MOLE 2.0.[20] Water channel (white) points toward the cytosolic environment, whereas solvent channel (blue) points above the lipid headgroups. All other channels point inside the bilayer. Channels 2e, 2c, and 3 point into the lipid headgroup region, whereas channels 4 and 2ac point below the lipid headgroups. Heme tilt angle θ (between heme plane and bilayer normal z, i.e., defined according to Baylon et al.[14]) is depicted.

debrisoquine) are immersed deeper in DOPC and palmitoyloleoylphophatidylglycerol (POPG) lipid bilayers than their corresponding CYP metabolites.[23] The metabolites also showed lower affinities for the membrane and higher penetration barriers than the substrates. These findings raise an important question as to whether the observed differences in membrane positions of CYP substrates correlate with the enzymes penetration depth, which in turn has implications for the metabolism of drugs.

In the present work, we compared orientations and immersion depths of six CYPs important for drug metabolism (CYP1A2, CYP2A6, CYP2C9, CYP2D6, CYP2E1, and CYP3A4). We constructed atomic models of the CYPs anchored to a DOPC bilayer and relaxed them using molecular dynamics simulations on a 100+ ns time scale. The constructed models agreed well with available experimental data as well as previously published models. We compared the orientations of the catalytic domains and positions of active site access channels of the different CYPs with respect to the lipid bilayer. Despite some differences between the orientation of individual CYPs on the membrane, all studied CYPs showed some common features, i.e., partial immersion of the catalytic domain (N-terminal part and part of F′/G′ loop) and a transmembrane N-terminal anchor attached to the catalytic domain via a loop. Entrances of active site access channels belonging to family 2 were generally positioned below the polar headgroup region of the lipid bilayer, whereas exits of the solvent channel were shifted toward the water−membrane interface. Positions of the active site access channels entrances corresponded closely with the lipid positions of substrates, whereas locations of the exits of the solvent channel correlated with the positions of metabolites. We concluded that channels from family 2 may be generally involved in substrate uptake to the CYP active site, especially of lipophilic substrates, whereas the solvent channel is likely to be involved in product release.

MATERIALS AND METHODS

Model Preparation. Structures of the catalytic domains were taken from the PDB database (Table S1, Supporting Information). Structures for the N-terminal anchor and native-like sequence were obtained by homology modeling using Modeller 9.10.[24] Two structural templates were used for each model. The catalytic domain was taken from the respective crystal structure and the missing N-terminal anchor from the atomic model of CYP2C9 equilibrated on a DOPC bilayer.[15]

Molecular Dynamics Settings. All models were immersed into dioleoylphosphatidylcholine (DOPC) lipid bilayers using the g_membed tool.[25] The Berger united atom force field for lipids[26] was used together with the G53a6 force field for proteins.[27] A physiological concentration of ions (0.1 M NaCl) in SPC/E water was used for solvation of the system. Overall, the simulation system consisted of around 90.000 united atoms in the case of CYP2C9 or around 120.000 united atoms in the case of other CYPs. Simulation of CYP2C9 from ref 15 was extended to 1 μs.

Gromacs 4.5.4 program package[28] was used for all MD simulations, applying a time step of 2 fs, a semi-isotropic Berendsen barostat at 1 bar, and V-rescale thermostat at 310 K. After energy minimization, the simulation was run with position restraints on the protein for 1 ns, followed by 10 consecutive 1 ns long simulations for system equilibration. Final MD simulations were run for 100 ns.

Analysis. The tilt angle between the heme plane, defined by the heme nitrogens, and the lipid bilayer normal, defined as the z axis, was analyzed over the last 50 ns of the production run.

Positions of the access/egress channels were calculated using the command-line version of the MOLE 2.0 software.[20] Analysis of the individual structures was also possible using the MOLEonline web server http://mole.upol.cz.[29] Analysis of the dynamical opening and closing of the channels was based on superimposed 1 ns snapshots from the last 50 ns of the simulations. Two types of simulations were considered: simulations of membrane-embedded CYP structures reported in this paper and CYP simulations in water reported in ref 30. Membrane atoms, as well as ions, waters, and hydrogens, were removed from the structures prior to channel computation. The interior threshold and bottleneck radius, which define the smallest detectable channels, were set to 1 Å. The probe radius and surface cover radius were set to 5 Å in order to sample the rough CYP surface. The starting point was set 4 Å above the heme iron. Snapshot structures were superimposed over the final structure of the catalytic domain. Central points of all channels were transcribed onto a 3D grid with 1 Å spacing in all directions. The maximal value of the radius at each point on the grid was selected. Only points with a radius larger than 1.5 Å (approximate radius of water) were reported. Positions of individual channel openings were defined as a series of channel points located on the surface of the protein.

RESULTS AND DISCUSSION

Model of Membrane-Bound CYP2C9: 1 μs Molecular Dynamics Simulation. The initial structure of CYP2C9 on the DOPC lipid bilayer was assumed to be the same as the model constructed in our previous study based on available experimental data.[15] A 1 μs long MD simulation of CYP2C9 on

dx.doi.org/10.1021/jp4059559 | J. Phys. Chem. B 2013, 117, 11556−11564

the membrane was carried out to test the simulation time required to achieve convergence of the orientation of CYP on the lipid bilayer. The catalytic domain fold remained stable, i.e., did not significantly deviate from the crystal structure (the root-mean-square deviation of 490 Cα atoms was smaller than 2.5 Å, Table S1, Supporting Information). Typical thermal fluctuations were detected mainly in the loops, similar to the fluctuations observed previously in MD simulations of the catalytic domain in water.[31]

However, the orientation of the catalytic domain with respect to the membrane relaxed during the course of the test simulation. The catalytic domain tilted from its initial orientation and spontaneously embedded deeper to the bilayer within the first 100 ns. Afterward, the orientation and penetration depth remained stable and did not significantly change further over the remainder of the 1 μs long MD simulation. As mentioned above, the fold of the catalytic domain remained stable and any fluctuations mostly occurred in the loops. The N-terminal helical anchor displayed a small precession movement around the membrane normal inside the lipid bilayer. The above findings suggested that a 100 ns long simulation was sufficient for obtaining a convergent model of CYP immersed in the lipid bilayer (Figure 2).

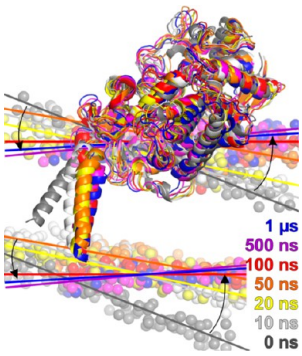

Figure 2. Position of CYP2C9 (represented by a secondary elements model) on a DOPC bilayer (only balls representing lipid phosphates are shown for clarity) showing that it converged on a 100 ns time scale and then remained stable until the end of the 1 μs long molecular dynamics (MD) simulation. Initial position of CYP2C9 was based on available experimental data and adopted from our previous study.[15] Snapshots extracted at different times (labeled on the right side) during the course of the MD simulation are superimposed over the catalytic domain to highlight the tilting of the initial structure (direction of tilting shown by black arrows).

All other CYP models (CYP1A2, CYP2A6, CYP2D6, CYP2E1, and CYP3A4) were constructed starting from the equilibrated structure of CYP2C9 taken after 100 ns. As expected, the bilayer orientation in these models converged even faster than in the CYP2C9 model, typically within the first 50 ns of the MD simulations (data not shown). During the MD simulations, the folds of all CYP catalytic domains remained stable except for typical thermal fluctuations. However, the depth and orientation in the membrane differed between the individual CYPs, as discussed below.

Immersion of the CYP2C9 catalytic domain in the membrane induced a funnel- or bowl-shaped depression in the lipid bilayer plane at the contact surface between CYP2C9 and bilayer (Figure 1). Due to the depression, the lipid headgroups and even water molecules shifted closer to the bilayer center than in the unperturbed bilayer (Figure S1, Supporting Information). In principle, four different CYP regions could be distinguished according to their interaction with the lipid bilayer: (i) region inside the lipid bilayer in contact with the nonpolar bilayer interior, (ii) region inside the lipid bilayer in contact with immersed polar headgroups, (iii) region above the lipid bilayer in contact with polar lipid headgroups, and finally (iv) region above the lipid bilayer in contact with the cytosol but not lipids.

Parts of the CYP2C9 catalytic domain that were completely immersed and in contact with the nonpolar lipid bilayer interior included the N-terminal transmembrane helix, tip of the β1 sheet, A′ helix, B′ helix in the B/C and F′/G′ loops, and N-terminal part of the G helix. However, a significantly larger part of the catalytic domain resided below the lipid bilayer surface plane, in contact with polar headgroups, i.e., large parts of the F and G helices, base of the B/C loop, and tip of the "finger" β4-β5 region. The third group consisted of parts lying above the membrane plane but still in contact with polar headgroups, i.e., the Pro-rich region connecting the N-terminal transmembrane helix with the catalytic domain, A helix, ends of the F and G helices, H/I loop, and majority of the "finger" β4-β5 region. The last group comprised parts mainly lying on the proximal side of the catalytic domain.

We analyzed the active site access channels using the recently developed MOLE 2.0 software, which has been shown to outperform previous software tools, e.g., CAVER 1.0[32] and MOLE 1.4.[33] Channels positioned around or through the F′/G′ loop (denoted 2a, 2ac, 2d, 2f, and 4 according to the nomenclature of Wade et al.[21]) and B′/C loop (2b, 2c, or 2e) would open their entrances into the headgroup region of the bilayer, but only channels 2b and 2c were detected open during the simulation. The channel leading between the F and the G helices (channel 3) would also point into the headgroup region. Just above the lipid headgroups, the solvent channel opened its exit and the water channel was found to be open to the proximal side facing the cytosol.

Membrane-Anchored CYPs: Common Features and Variations. Molecular dynamics simulations of CYP models other than CYP2C9 showed quicker convergence of their orientation on the lipid bilayer, most likely because their initial positions were based on the relaxed position of CYP2C9 on the bilayer. All studied CYPs had catalytic domains that were partially immersed in the bilayer, like CYP2C9; however, they displayed slightly different and CYP-specific orientations and immersions (Figures 3 and 4).

The common parts immersed in the nonpolar regions of the membrane were the transmembrane helical anchor, loop of the A′ helix, and the F′ and G′ helices. Parts below the bilayer plane but still in contact with polar headgroups of the lipids were the most variable. They reflected individual and specific CYP orientations on the lipid bilayer (discussed in detail later). The F/G loop displayed contact with the membrane interior, and its tip reached the membrane center. The H/I loop and "finger" β4−5 region were in contact with the polar headgroups but above the bilayer. The proline-rich region lies above the membrane plane due to the rather high polarity of adjacent amino acids. As a consequence, the arrangement of the membrane-anchoring region was as follows: transmembrane N terminal helix, followed by the rather polar Pro-rich region in contact with the water−membrane interface, followed by the A′ helix loop (in cases where it could occur), which was immersed in the membrane. The subsequent A helix was in all cases just above the polar headgroups. Such an arrangement was the

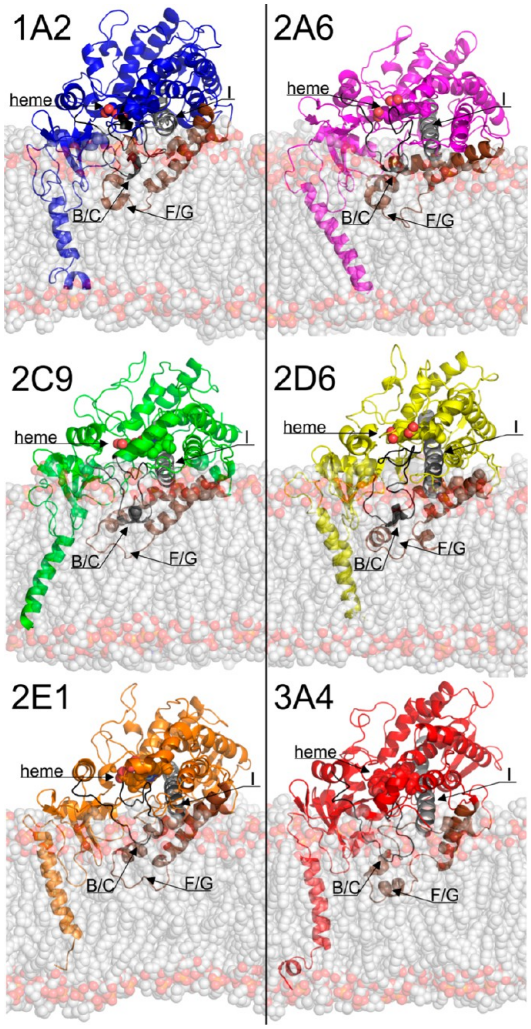

Figure 3. Final snapshots of membrane-anchored CYPs from molecular dynamics simulations showing their orientations on the lipid bilayer. All structures were oriented horizontally with respect to the bilayer plane and perpendicularly with respect to I helix in-plane vector (shown in gray). Different orientations of CYPs can be easily seen from the variation of the tilting angles of I helix with respect to the membrane plane. B/C and F/G loops are shown in black and brown, respectively. As the whole lipid bilayer is shown in a transparent mode, only the frontmost layer of the lipid molecules are visible, and therefore, the membrane depression of the lipids closer to the CYP is partially hidden in this visualization by unperturbed bilayer in front. Water molecules are not shown for clarity.

common membrane anchorage for all studied CYP catalytic domains (Figure 5), but slight differences in immersion and orientation were detected between the individual CYPs.

The individual CYP models on lipid bilayers also displayed some variations in orientation and penetration depth on the lipid bilayer. The orientation of CYP on the membrane can be experimentally characterized by measurement of the tilt angle θ (shown in Figure 1) between the heme plane and the lipid bilayer normal.[13] A tilt angle θ of $(60 \pm 4)^\circ$ has recently been measured for CYP3A4 in POPC nanodiscs by linear dichroism.[14] The tilt angle calculated from the last 50 ns of our MD simulation was $(56 \pm 5)^\circ$, which agrees with the experimental value within error bars. The MD simulations showed that the tilt angle values varied among the studied CYPs (Table 1), ranging from 56° (CYP3A4) to 72° (CYP2D6). Tajkhorshid et al.[14] predicted a tilt angle of $(72 \pm 3)^\circ$ for CYP3A4 from MD simulations, but this value differed significantly from the experimental value reported in the same paper. This difference can be attributed to the membrane model (highly mobile membrane model, HMMM) used in the respective article. HMMM consists of two distinctive parts: (i) short lipid tails combined with dichloroethane (to increase the mobility of the membrane interior and thereby convergence of the protein model while retaining the lipid bilayer polarity and density profiles) and (ii) carbonyl groups constrained to their specific positions in the unperturbed membrane to retain the size of the respective membrane. However, the latter constraint does not allow deformation of the CYP/membrane interface (cf. Figure 1) and consequently may prohibit deeper immersion of CYP into the HMMM membrane.

Our simulations showed that the D/E loop of *CYP1A2* was more inclined toward the membrane than that of CYP2C9. Consequently, the β1 sheet and B/C loop of CYP1A2 were pulled out of the membrane while still retaining some contact with head groups (Figure 3). The F/G loop was immersed below the lipid headgroups, thus allowing channels in its vicinity (2a, 2f, 4) to open into the interior of the lipid bilayer, but these channels were not observed during the simulation. Only channels pointing into the headgroup region were observed between the B/C and the F/G loops (2c) and between the F/G loop and the I helix (S)). A channel pointing toward the proximal side (water channel) opened toward the cytosol (Figure 6).

CYP2A6 adopted a similar orientation in the membrane to that of CYP1A2. The only difference was slightly greater immersion of the B′ and G helices of CYP2A6 (Figure 3). The positions of the channel openings of CYP2A6 were therefore similar to those discussed in the previous paragraph. The main differences were that channels in the vicinity of the B/C loop were immersed deeper to the bilayer (2c), the channel through the F/G loop (4) pointed toward the lipid bilayer interior, and the remaining channel (2b, S) pointed toward the lipid head groups (Figure 6).

Of all the CYPs studied, *CYP2D6* differed in the orientation such that its F and G helices and beta "finger" β4−5 loop had the smallest contact with the membrane, which meant that the solvent channel had low contact with the membrane and opened into the cytosol (Figure 3). The D/E loop also had no contact with the membrane; therefore, CYP2D6 had the smallest contact surface with the membrane. On the other hand, the B/C loop had extensive contact with the nonpolar part of the membrane, thus making channels in its vicinity more immersed than in other CYPs and in contact with lipids (2c, 2b, 2e). Also, the tip of the F/G loop pointed toward the nonpolar interior of the bilayer. Therefore, channels in its vicinity (4, 2f) were accessible from the membrane interior (Figure 6).

The orientation of *CYP2E1* was similar to CYP2D6, but it was slightly more immersed as it made larger contact with the membrane facilitated by the beta "finger" β4−5 region (Figure 3). Only the B′ helix of the B/C loop was immersed below the lipid headgroups, and therefore, only a channel through the F/G loop contacted the nonpolar part of the membrane (2f). The rest of the channels around the B/C loop (2c, 2b, 2e) pointed to lipid headgroups, and the solvent channel pointed more to the cytosol (Figure 6).

CYP3A4 exhibited the most similar orientation and immersion to those of CYP2C9. However, CYP3A4 has more polar amino acids in the anchorage region, as shown by its

dx.doi.org/10.1021/jp4059559 | J. Phys. Chem. B 2013, 117, 11556−11564

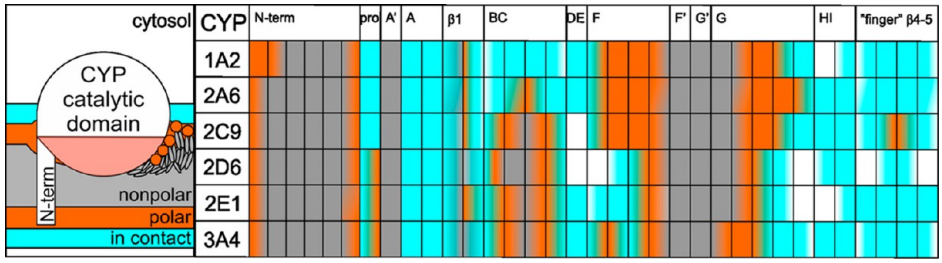

Figure 4. Comparison of immersion and orientation of different regions in equilibrated cytochrome P450 structures. Schematic representation of a CYP on a membrane is shown in the left panel. Lipids on the protein−membrane interface adopt a specific arrangement, as shown in the schematic. Some parts of the CYP are in contact with polar lipid headgroups on the membrane surface (blue). Lipid headgroups in the vicinity of the protein lie below the membrane surface due to interactions with polar residues (orange), and part of the CYP catalytic domain is immersed below the membrane plane (red). In contrast, only a small part of the catalytic domain below the membrane surface interacts with the nonpolar center of the membrane (gray). Right panel displays the positions of important CYP regions in the bilayer (cf. the left panel for color coding).

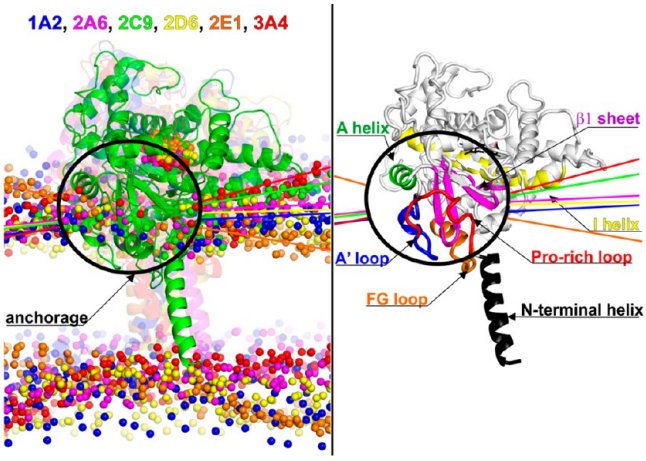

Figure 5. CYP N-terminal anchorage region. Catalytic domains of all final CYP structures on bilayers are shown superimposed. Phosphorus atoms are represented by spheres of different colors for the individual CYPs (CYP1A2, blue; 2A6, magenta; 2C9, green; 2D6, yellow; 2E1, orange; 3A4, red). Pro-rich region followed by a deeply immersed nonpolar loop was found to be the common anchor region in all CYP structures with similar immersion, whereas catalytic domains displayed different degrees of immersion and orientation.

Table 1. Tilt Angle (in degrees) between the Heme Plane and the Lipid Bilayer Normal (cf. Figure 1)

CYP	simulation	experiment	literature[a]
1A2	67 ± 6		
2A6	69 ± 5		
2C9	61 ± 4		55 ± 5,[15] 50 or 35[16]
2D6	72 ± 6		
2E1	60 ± 5		
3A4	56 ± 5	60 ± 4[14]	72 ± 3[14]

[a]Values were recalculated to match the angle between the heme plane and the membrane normal as defined in ref 14.

hydration pattern reported by Hendrychova et al.[30] Thus, CYP3A4 makes greater contact with the polar headgroups despite having similar immersion to that of CYP2C9. The parts in contact with the nonpolar part of the bilayer included the A′ loop, part of the B/C loop, and the whole F/G loop. The parts in contact with the polar headgroups below the membrane plane were the Pro-rich region, β1 sheet, B/C loop, and F and G helices. The D/E and H/I loops remained above the plane, retaining contact with the polar headgroups. However, the

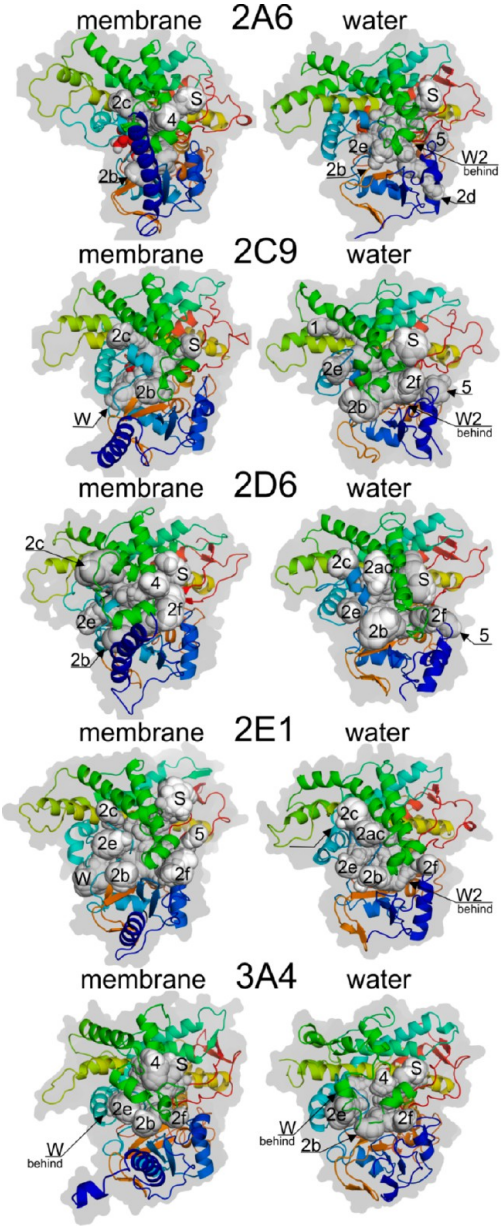

Figure 6. Open channels detected in the CYP membrane (left) and water (right) simulations. Only channels wide enough to enable passage of a probe of radius 1.5 Å are shown.

dx.doi.org/10.1021/jp4059559 | J. Phys. Chem. B 2013, 117, 11556−11564

"finger" $\beta4-\beta5$ region was less immersed in the membrane than in the case of CYP2C9 (Figure 3). The channels that opened in contact with the hydrophobic part of the membrane were all located around the F/G loop (2f, 2b, 4). Channel 2e and the solvent channel opened just above the lipid headgroups. Finally, the water channel pointed directly into the cytosol (Figure 6).

Analysis of CYPs' surface amino acids showed that 12.5% of the surface was in contact with lipid tails, 36.5% faced the lipid headgroups, and 51% of the surface amino acids faced cytosolic water. Aliphatic (V, I, L) and nonpolar phenylalanine (F) and cysteine (C) amino acids occurred preferentially on the contact surface with the lipid tails, whereas all charged (R, K, D, E) and polar amino acids (H, Q) and glycine (G) were underpopulated in this contact region (Tables S2 and S3, Supporting Information). The contact surface with the headgroup region contained a higher amount of tryptophan (W), lysine (K), and glutamine (Q) amino acids, whereas some nonpolar amino acids (I, F, and C) were underpopulated. Charged amino acids (K, R, D) were overpopulated on the cytosolic surface, whereas nonpolar amino acids (V, L, W) were underpopulated in this area. The observed differences in membrane orientations of individual CYPs can be rationalized by different amino acids composition of CYP surfaces. CYPs surface spots rich in nonpolar aliphatic amino acids push these parts toward the membrane interior, while tryptophan to the interface and charged amino acids prefer to be immersed in either the headgroup region or cytosol.

Behavior of Active Site Access/Egress Channel Network in Membrane-Anchored and Solvent-Exposed CYPs. The mechanism of substrate and product channeling to and out of the CYP active site is an important but still not fully answered question of CYP structural biology. Because of a lack of direct experimental data, clues as to the mechanism of substrate/product channeling have relied on analyses of X-ray structures[21,34] and MD simulations.[3,34−39] However, recent models of membrane-anchored CYP2C9 have identified significant differences in the behavior of membrane-anchored and fully solvent-exposed enzyme.[15,16] Phospholipids have been shown to enhance the activity of ethoxyresorufin-*O*-deethylase in recent experiments by Ghosh and Ray.[40] Thus, to test whether this also applies to CYPs, we compared the behavior of membrane-anchored and fully solvent-exposed CYPs. We focused on the access channels, which were analyzed using a recent version of MOLE 2.0 software. For comparison, CYP MD simulations in water were taken from ref 30 and analyzed using the same protocol.

We found that the channels fluctuated dynamically (opened and closed) during the course of the MD simulations. In contrast, in most of the reported CYP X-ray structures, the channels appear to be closed as they usually have radii below 1.4 A. If the channels were rigid, passage of CYP substrates to the active site would be hindered because CYP substrates are typically larger than the diameter of the channel bottlenecks. However, if the channels fluctuate (breathe) over time, as the MD simulations imply, molecules may enter and leave the CYP active site. Therefore, the bottleneck can move along the channel line as a "peristaltic wave", allowing molecules to pass through the active site access/egress channel. The same mechanism has already been reported for passage of water molecules to CYP active sites.[30] In addition, adaptive changes in the local channel cross-section may also be induced by the presence of a ligand in the channel. It should be noted that large conformational changes of the CYP catalytic domain may also occur, e.g., as observed for CYP2B4, leading to wide opening of the CYP2B4 active site.[41] However, these changes are unlikely to be detected in MD simulations due to the still short time scales used (hundreds of nanoseconds).

The membrane-bound CYPs showed fewer open channels than the same CYPs simulated in water (Figure 6 and Table 2).

Table 2. CYP Channels (denoted according to the nomenclature by Wade et al.[21]) Having Radius Above 1.5 Å Calculated from MD Simulations in the Membrane (this work) and Water (taken from ref 1) by MOLE 2.0 Software[a]

CYP	membrane	water
1A2	**S**, 2c, W	N.A.
2A6	S, 2b, 2c, 4	S, 2b, 2d, 2e, 5, W2
2C9	S, 2b, 2c, **W**	S, 2b, 2e, 2f, 1, 5, W2
2D6	S, 2b, **2c**, **2e**, **2f**, **4**	S, 2b, 2c, 2e, 2f, 2ac, 5
2E1	**S**, 2b, 2c, **2e**, 2f, 5, W	2b, 2c, 2e, 2f, 2ac
3A4	**S**, 2b, **2e**, 2f, 4, W	S, 2b, 2e, 2f, 4, W

[a]In **bold** are highlighted channels with radius above 2 Å. MD simulation of CYP1A2 in water was not carried out.

This can be attributed to smaller fluctuations of the membrane-exposed parts of catalytic domains in comparison with solvent-exposed parts of the catalytic domains or when exposed only to a water environment, as movements of protein chains are slower in lipids than in water.[15,16] The most open CYP structures (having channels with the largest bottleneck radii) were CYP3A4, CYP2D6, and CYP2E1, which also had the most channels opening toward the membrane interior. In contrast, CYP1A2 had the most closed structure. The solvent channel and channel 2b were detected in both the water and the membrane simulations; the former typically had a larger bottleneck radius than the corresponding channel 2b. Open channels 2c and 4 were present more frequently in membrane simulations than in the water simulations, whereas open channels 2e and 2f were preferentially found in the water simulations. It should be noted that open channels 2e and 2f were only identified in the membrane simulation of the most open CYPs (CYP3A4, CYP2D6, and CYP2E1). Channel 5 was closed in all membrane simulations but open in most simulations in water. Channels 1, 2ac, and 2d were open only in the water simulations. On the other hand, the water channel (running from the active site between the I helix and heme and opening on the proximal side) was closed in the water simulations but open in most of the membrane simulations. Thus, the lipid environment resulted in closure of channels 5, 1, and 2d and the water channel. Channels belonging to the 2x family (mostly channels 2b and 2c) were open and had entrances in/below the headgroup region. The solvent channel pointed just above the lipid headgroups, and the water channel opened to the cytosol. Finally, CYPs on the membrane more often had an open channel 4 pointing toward the lipid tails.

In summary, MD simulations showed the dynamic character of the active site access channels, many of which fluctuated (opened and closed) during the course of the simulations. Further, the active site access channel networks differed between the water and the membrane environments, indicating that only data on membrane-anchored CYPs is relevant for determining the substrate/product channeling mechanism in vivo.

dx.doi.org/10.1021/jp4059559 | J. Phys. Chem. B 2013, 117, 11556−11564

Comparison of Positions of Access/Egress Active Site Openings with Penetration Depths of Prototypical CYP Substrates and Metabolites. Simulation results showed that CYPs anchored to a membrane have complex networks of active site access and egress channels, with some opening their entrances inside the membrane while others opening at/above the water−membrane interface. As the orientations of the catalytic domains differ between the individual CYPs, the exact positioning of channel entrances reflects the specific orientation of the individual CYP (Figure 7). Generally, substrates and

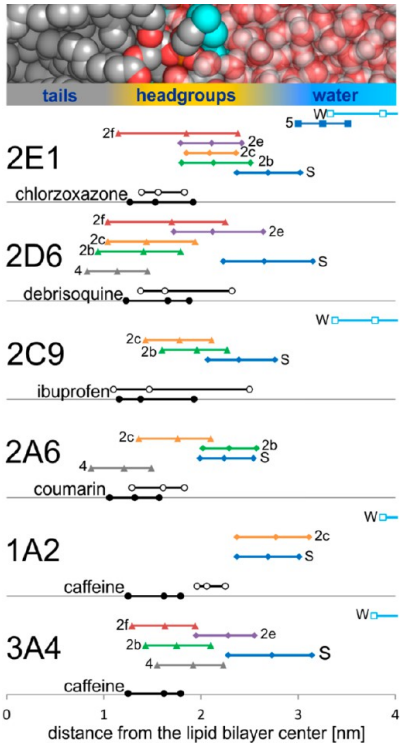

Figure 7. Scheme showing the positions of substrates (filled black circles; central circle represents ligand's center-of-mass membrane position with the lowest free energy, and right and left circles delimit the area accessible at RT, T = 310 K) and their respective metabolites (open circles). Average, minimal, and maximal positions of CYP active site access/egress channels openings (denoted according to the nomenclature of Wade et al.[21]) in the membrane were calculated as centers of balls inscribed in the channel's openings. Substrate access channels whose membrane positions overlap with positions of substrates are shown by triangles, while product release channels (i.e., channels whose membrane positions overlap with positions of metabolites) are shown by diamonds. Channels pointing toward the cytosol are shown by squares. (Top) Membrane profile on the same scale for ready comparison.

metabolites localize in the membrane layer, where channel openings are also positioned. Nevertheless, most substrates tend to be closer to the nonpolar phospholipid tail region (deeper in the membrane), whereas most metabolites tend to be closer to the water−membrane interface because metabolites are usually less lipophilic than their respective substrates (cf. Figure S2, Supporting Information).[23] It should be noted that substrates also typically have higher affinities for the membrane than the respective metabolites.[23] The differences in affinities and positioning of substrates and metabolites may generate concentration gradients that are crucial for CYP action, i.e., the high affinity of substrates may enhance the local concentration of the substrate in the membrane, whereas the low affinity of metabolites may facilitate membrane clearance (release of the respective metabolite to the cytosol for subsequent metabolic steps). In addition, as the membrane positions of the studied substrates correlate with the openings of the active site access channels from the family 2x, we may infer that these channels are involved in substrate trafficking to the CYP active site. On the other hand, as metabolites tend to be positioned near the water−membrane interface where the opening of the solvent channel is located, we may surmise that the solvent channel is involved in product release.

Another important question concerns whether the positions of substrate access channels correlate with substrate preferences of individual CYPs. Some channels retained similar membrane positions in most of the studied CYPs, whereas others varied more significantly. The channels that always pointed toward the lipid interior were channels 2f and 4, which may therefore serve as common access channels for lipophilic substrates. The solvent channel always pointed into the water−membrane interface and therefore may serve as an entrance/release for hydrophilic substrates/products. However, the positions of some channels from the 2x family differed considerably. For instance, channel 2b was inserted deep into the lipid bilayer in CYP3A4, CYP2C9, and CYP2D6, whereas it pointed toward the water−membrane interface in CYP2A6 and CYP2E1. The differences observed in the channel opening positions reflect the variability of the amino acid composition of the region, which is in contact with the membrane.

We also identified variations in amino acid composition in openings of each channel type (Table S4, Supporting Information). The W channel had the least variable channel openings, which were positively charged due to the presence of arginine(s). Solvent channel openings were polar with at least two polar amino acids in all CYPs; however, they contained a variable number of nonpolar amino acids, which was compensated with charged ones. Amino acid composition of other channels was more specific for individual CYPs. Openings of channels 2b and 2c also contained polar or charged amino acids in their openings, but the numbers of nonpolar amino acids present there were larger in channel 2c in CYP1A2 and CYP2C9. Channel 2e openings contained a relatively large amount of charged amino acids. Openings of channels 2f and 4, on the other hand, were rather nonpolar however not in all cases, e.g., CYP2D6 was an exception. Comparing amino acids composition of opening CYP active site access channels we observe the same common features (like the charged W channel and rather polar solvent channel) as well as variations among individual CYPs. This indicates that the composition of channel openings may also contribute to substrate preferences of individual CYPs.

Taking into account the predicted fluctuations of the CYP catalytic domain on the membrane, the thermally accessible space of the substrate in the membrane, and the number (and variability) of CYP substrates, it seems unlikely that there is a straightforward correlation between substrate membrane positions and CYP substrate preferences. However, most membrane-anchored CYPs have probably evolutionarily adapted for flexible uptake of lipophilic substrates from membranes and release of the more hydrophilic metabolites to a membrane−water interface or the cytosol. Nevertheless, we cannot rule out the possibility that some CYP forms (e.g., CYP3A4) may also uptake more hydrophilic substrates directly from the water−membrane interface.

CONCLUSIONS

Human microsomal cytochromes P450 are membrane-anchored enzymes significantly involved in drug metabolism. While a wealth of structural information about water-soluble engineered CYPs has been obtained from X-ray crystallography, information about the membrane orientation and immersion has so far been limited. In this study, we constructed atomic models of several membrane-anchored human CYPs known to be involved in drug metabolism (CYPs 1A2, 2A6, 2C9, 2D6, 2E1, and 3A4). We relaxed the atomic models by MD simulation on a 100+ ns time scale. We showed that the region of the trans-membrane helix attachment to the catalytic site ("anchorage region") is similarly immersed in the membrane for all CYP models studied, whereas the catalytic domains generally differ in their orientation toward the membrane, as shown by the different heme tilt angles. The heme tilt angle calculated from the MD simulation of membrane-anchored CYP3A4 $(56 \pm 5)^\circ$ was in agreement with a recently reported experimental value $(60 \pm 4)^\circ$. The lipid bilayer was also influenced by the presence of CYP. In particular, it adopted a funnel- or bowl-like deformation at the enzyme/membrane interface, causing the polar head groups to shift closer to the lipid bilayer center. Comparison of the behavior of fully water-exposed and membrane-anchored CYP showed that the lipid environment also influences the opening of channels. The six forms of membrane-anchored CYP studied here shared several common features, e.g., a catalytic domain partially immersed in the membrane with a solvent-exposed proximal side. However, the orientation of individual CYPs on the membrane displayed some variations. We thoroughly analyzed the network of active site access and egress channels. The opening of channels belonging to the 2x family faced either the membrane interior or the membrane head groups, whereas the solvent channel pointed to the water−membrane interface. We further compared the positions of access and egress channels openings with positions of prototypical CYP substrates and their respective metabolites. The results suggested that the deeply immersed channel openings may facilitate uptake of lipophilic substrates from the membrane to the active site, whereas the solvent channel serves as an entrance or exit for more hydrophilic substrates or products. Our data also indicate that the amino acid composition of access channels openings may contribute to substrate preferences of individual CYPs.

ASSOCIATED CONTENT

Supporting Information

Details about setup and RMSD of catalytic domains, amino acids composition of CYPs surface parts in contact with membrane, headgroup, and cytosol and access channels openings, and supporting figures showing bilayer density profile and prototypical free energy profiles along membrane normal. This material is available free of charge via the Internet at http://pubs.acs.org.

AUTHOR INFORMATION

Corresponding Author

*E-mail: michal.otyepka@upol.cz.

Notes

The authors declare no competing financial interest.

ACKNOWLEDGMENTS

This work has been supported by the Operational Program Research and Development for Innovations - European Regional Development Fund (CZ.1.05/2.1.00/03.0058) and Operational Program Education for Competitiveness - European Social Fund (CZ.1.07/2.3.00/20.0017 and /20.0058). M.O. acknowledges support by the Czech Grant Agency through the P208/12/G016 project. K.B. acknowledges support by the Czech Grant Agency through the P303/12/P019 project. M.P. acknowledges support by the student project PrF_2013_028 (Palacký University Olomouc).

REFERENCES

(1) Black, S. D. Membrane Topology of the Mammalian P450 Cytochromes. *FASEB J.* **1992**, *6*, 680−685.

(2) Johnson, E. F.; Stout, C. D. Structural Diversity Of Eukaryotic Membrane Cytochromes P450. *J. Biol. Chem.* **2013**, *288*, 17082−17090.

(3) Otyepka, M.; Berka, K.; Anzenbacher, P. Is There a Relationship Between the Substrate Preferences and Structural Flexibility of Cytochromes P450? *Curr. Drug Metab.* **2012**, *13*, 130−142.

(4) Domanski, T. L.; Halpert, J. R. Analysis of Mammalian Cytochrome P450 Structure and Function by Site-directed Mutagenesis. *Curr. Drug Metab.* **2001**, *2*, 117−37.

(5) Poulos, T.; Johnson, E. Structures of cytochrome P450 enzymes. In *Cytochrome P450: Structure, Mechanism, and Biochemistry*; Ortiz de Montellano, P. R., Ed.; Kluwer Academic/Plenum Publishers: New York, 2005; pp 87−114.

(6) Otyepka, M.; Skopalík, J.; Anzenbacherová, E.; Anzenbacher, P. What Common Structural Features and Variations of Mammalian P450s Are Known to Date? *Biochim. Biophys. Acta, Gen. Subj.* **2007**, *1770*, 376−389.

(7) Brown, C. A.; Black, S. D. Membrane Topology of Mammalian Cytochromes P-450 from Liver Endoplasmic Reticulum. Determination by Trypsinolysis of Phenobarbital-treated Microsomes. *J. Biol. Chem.* **1989**, *264*, 4442−9.

(8) von Wachenfeldt, C.; Johnson, E. F. Structures of Eukaryotic Cytochrome P450 Enzymes-Membrane Topology. In *Cytochrome P450: Structure, Mechanism and Biochemistry*; Plenum Press: New York, 1995; pp 183− 223.

(9) Ozalp, C.; Szczesna-Skorupa, E.; Kemper, B. Bimolecular Fluorescence Complementation Analysis of Cytochrome P450 2c2, 2e1, and NADPH-cytochrome P450 Reductase Molecular Interactions in Living. *Drug Metab. Dispos.* **2005**, *33*, 1382−1390.

(10) Headlam, M. J.; Wilce, M. C. J.; Tuckey, R. C. The F-G Loop Region of Cytochrome P450scc (CYP11A1) Interacts with the Phospholipid Membrane. *Biochim. Biophys. Acta, Biomembr.* **2003**, *1617*, 96−108.

(11) Kiselyova, O. I.; Yaminsky, I. V; Ivanov, Y. D.; Kanaeva, I. P.; Kuznetsov, V. Y.; Archakov, A. I. AFM Study of Membrane Proteins, Cytochrome P450 2B4, and NADPH-cytochrome P450 Reductase and Their Complex Formation. *Arch. Biochem. Biophys.* **1999**, *371*, 1−7.

(12) Nussio, M. R.; Voelcker, N. H.; Miners, J. O.; Lewis, B. C.; Sykes, M. J.; Shapter, J. G. AFM Study of the Interaction of Cytochrome P450 2C9 with Phospholipid Bilayers. *Chem. Phys. Lipids* **2010**, *163*, 182−189.

(13) Ohta, Y.; Kawato, S.; Tagashira, H.; Takemori, S.; Kominami, S. Dynamic Structures of Adrenocortical Cytochrome P-450 in Proteoliposomes and Microsomes: Protein Rotation Study. *Biochemistry* **1992**, *31*, 12680−12687.

(14) Baylon, J. L.; Lenov, I. L.; Sligar, S. G.; Tajkhorshid, E. Characterizing the Membrane-Bound State of Cytochrome P450 3A4: Structure, Depth of Insertion and Orientation. *J. Am. Chem. Soc.* **2013**, *135*, 8542−8551.

(15) Berka, K.; Hendrychová, T.; Anzenbacher, P.; Otyepka, M. Membrane Position of Ibuprofen Agrees with Suggested Access Path

Entrance to Cytochrome P450 2C9 Active Site. *J. Phys. Chem. A* **2011**, *115*, 11248−11255.
(16) Cojocaru, V.; Balali-Mood, K.; Sansom, M. S. P.; Wade, R. C. Structure and Dynamics of the Membrane-bound Cytochrome P450 2C9. *PLoS Comput. Biol.* **2011**, *7*, e1002152.
(17) Denisov, I. G.; Shih, a Y.; Sligar, S. G. Structural Differences Between Soluble and Membrane Bound Cytochrome P450s. *J. Inorg. Biochem.* **2012**, *108*, 150−158.
(18) Sgrignani, J.; Magistrato, A. Influence of the Membrane Lipophilic Environment on the Structure and on the Substrate Access/egress Routes of the Human Aromatase Enzyme. A Computational Study. *J. Chem. Inf. Model.* **2012**, *52*, 1595−1606.
(19) Jiang, W.; Ghosh, D. Motion and Flexibility in Human Cytochrome P450 Aromatase. *PloS ONE* **2012**, *7*, e32565.
(20) Sehnal, D.; Svobodová Vařeková, R.; Berka, K.; Pravda, L.; Navrátilová, V.; Banáš, P.; Ionescu, C.-M.; Geidl, S.; Otyepka, M.; Koča, J. MOLE 2.0: Advanced Approach for Analysis of Biomacromolecular Channels. *J. Cheminform.* **2013**, *5*, 39.
(21) Cojocaru, V.; Winn, P. J.; Wade, R. C. The Ins and Outs of Cytochrome P450s. *Biochim. Biophys. Acta* **2007**, *1770*, 390−401.
(22) Conner, K. P.; Woods, C. M.; Atkins, W. M. Interactions of Cytochrome P450s with Their Ligands. *Arch. Biochem. Biophys.* **2011**, *507*, 56−65.
(23) Paloncýová, M.; Berka, K.; Otyepka, M. Molecular Insight into Affinities of Drugs and Their Metabolites to Lipid Bilayers. *J. Phys. Chem. B* **2013**, *117*, 2403−2410.
(24) Sali, A.; Blundell, T. L. Comparative Protein Modelling by Satisfaction of Spatial Restraints. *J. Mol. Biol.* **1993**, *234*, 779−815.
(25) Wolf, M. G.; Hoefling, M.; Aponte-Santamaría, C.; Grubmüller, H.; Groenhof, G. G_membed: Efficient Insertion of a Membrane Protein into an Equilibrated Lipid Bilayer with Minimal Perturbation. *J. Comput. Chem.* **2010**, *31*, 2169−2174.
(26) Berger, O.; Edholm, O.; Jähnig, F. Molecular Dynamics Simulations of a Fluid Bilayer of Dipalmitoylphosphatidylcholine at Full Hydration, Constant Pressure, and Constant Temperature. *Biophys. J.* **1997**, *72*, 2002−2013.
(27) Oostenbrink, C.; Villa, A.; Mark, A. E.; Gunsteren, W. F.; Van, A. Biomolecular Force Field Based on the Free Enthalpy of Hydration and Solvation: The GROMOS Force-Field Parameter Sets 53A5 and 53A6. *J. Comput. Chem.* **2004**, *25*, 1656−1676.
(28) Hess, B.; Kutzner, C.; van der Spoel, D.; Lindahl, E. GROMACS 4: Algorithms for Highly Efficient, Load-Balanced, and Scalable Molecular Simulation. *J. Chem. Theory Comput.* **2008**, *4*, 435−447.
(29) Berka, K.; Hanák, O.; Sehnal, D.; Banáš, P.; Navrátilová, V.; Jaiswal, D.; Ionescu, C.-M.; Svobodová Vařeková, R.; Koča, J.; Otyepka, M. MOLEonline 2.0: Interactive Web-based Analysis of Biomacromolecular Channels. *Nucleic Acids Res.* **2012**, *40*, W222−W227.
(30) Hendrychová, T.; Berka, K.; Navrátilová, V.; Anzenbacher, P.; Otyepka, M. Dynamics and Hydration of the Active Sites of Mammalian Cytochromes P450 Probed by Molecular Dynamics Simulations. *Curr. Drug Metab.* **2012**, *13*, 177−189.
(31) Skopalík, J.; Anzenbacher, P.; Otyepka, M. Flexibility of Human Cytochromes P450: Molecular Dynamics Reveals Differences Between CYPs 3A4, 2C9, and 2A6, Which Correlate with Their Substrate Preferences. *J. Phys. Chem. B* **2008**, *112*, 8165−8173.
(32) Petřek, M.; Otyepka, M.; Banáš, P.; Košinová, P.; Koča, J.; Damborský, J. CAVER: a New Tool to Explore Routes from Protein Clefts, Pockets and Cavities. *BMC Bioinf.* **2006**, *7*, 316.
(33) Petřek, M.; Košinová, P.; Koča, J.; Otyepka, M.; Petrek, M.; Kosinová, P.; Koca, J. MOLE: a Voronoi Diagram-based Explorer of Molecular Channels, Pores, and Tunnels. *Structure* **2007**, *15*, 1357−1363.
(34) Fishelovitch, D.; Shaik, S.; Wolfson, H. J.; Nussinov, R. Theoretical Characterization of Substrate Access/exit Channels in the Human Cytochrome P450 3A4 Enzyme: Involvement of Phenylalanine Residues in the Gating Mechanism. *J. Phys. Chem. B* **2009**, *113*, 13018−13025.
(35) Wade, R. C.; Winn, P. J.; Schlichting, I.; Sudarko, A. Survey of Active Site Access Channels in Cytochromes P450. *J. Inorg. Biochem.* **2004**, *98*, 1175−1182.
(36) Schleinkofer, K.; Winn, P. J.; Lüdemann, S. K.; Wade, R. C. Do Mammalian Cytochrome P450s Show Multiple Ligand Access Pathways and Ligand Channelling? *EMBO Rep.* **2005**, *6*, 584−589.
(37) Li, W.; Liu, H.; Luo, X.; Zhu, W.; Tang, Y.; Halpert, J. R.; Jiang, H. Possible Pathway(s) of Metyrapone Egress from the Active Site of Cytochrome P450 3A4: a Molecular Dynamics Simulation. *Drug Metab. Dispos.* **2007**, *35*, 689−696.
(38) Li, W.; Shen, J.; Liu, G.; Tang, Y.; Hoshino, T. Exploring Coumarin Egress Channels in Human Cytochrome P450 2A6 by Random Acceleration and Steered Molecular Dynamics Simulations. *Proteins* **2010**, *79*, 271−281.
(39) Krishnamoorthy, N.; Gajendrarao, P.; Thangapandian, S.; Lee, Y.; Lee, K. W. Probing Possible Egress Channels for Multiple Ligands in Human CYP3A4: a Molecular Modeling Study. *J. Mol. Model.* **2010**, *16*, 607−614.
(40) Ghosh, M. C.; Ray, A. K. Membrane Phospholipid Augments Cytochrome P4501a Enzymatic Activity by Modulating Structural Conformation During Detoxification of Xenobiotics. *PloS ONE* **2013**, *8*, e57919.
(41) Wilderman, P. R.; Halpert, J. R. Plasticity of CYP2B Enzymes: Structural and Solution Biophysical Methods. *Curr. Drug Metab.* **2012**, *13*, 167−176.